Direct Atomic Force Microscopic Determination of Surface Charge at the Gold/Electrolyte Interface—The Inadequacy of Classical GCS Theory in Describing the Double-Layer Charge Distribution

Jian Wang and Allen J. Bard*

Department of Chemistry and Biochemistry, University of Texas at Austin, Austin, Texas 78712

Received: October 6, 2000; In Final Form: January 23, 2001

The surface charge at the interface of a Au electrode with a $KClO_4$ solution was measured by in situ atomic force microscopy (AFM) using a modified cantilever with a charged SiO_2 sphere. The effective charge determined by treating the AFM force curve was much smaller than that injected electrochemically, with the ratio of the effective/real surface charge to the electrochemical charge being below 10%. This large difference suggests that classical Gouy−Chapman−Stern (GCS) theory is inadequate to describe the diffuse electrical double layer. Ion correlation and ion condensation effects might account for the reduced surface charge. Additional experiments on the effect of electrolytes containing divalent species [$Ca(NO_3)_2$ and Na_2SO_4] and the effect of adsorption of sodium dodecyl sulfate on the Au electrode provide additional evidence for such effects.

Introduction

Many experiments and theoretical treatments have addressed the charge distribution at the solid (e.g., metal electrode or colloidal particle)/electrolyte interface. For charged surfaces, the surface charge is balanced by an equal and opposite net charge of ions in the electrolyte. The spatial separation of charge in the electrolyte is termed the electrical double layer. The electrical double layer plays a key role in many processes, e.g., the stability of colloidal dispersions, the formation of bilayer membranes, and the transport of ions and other molecules across cell membranes. The charge on the surface is a crucial quantity in physical and colloid chemistry and biophysics that determines the properties of the electrical double layer.

In electrochemistry, the charge and potential distribution at the electrode solution interface is most often described by the classical Guoy−Chapman−Stern (GCS) model,[1] although there has been extensive work on alternative models of the double layer. In the GCS model the interface is described in terms of a compact (Helmholtz) layer, which in the absence of specific adsorption contains only solvent molecules, and a diffuse layer where the charge distribution is calculated by solution of the Poisson−Boltzmann (PB) equation. The locus of centers of the ions at the position of closest approach is called the outer Helmholtz plane (OHP), taken at the position x_2, and the inner potential at that plane is designated as ϕ_2 (or sometimes as the outer potential ψ_2). The GCS model provides an equation that relates the total charge in the diffuse layer, σ^S (which is equal to $-\sigma^M$, the charge on the metal electrode), to ϕ_2.

During the past several decades, a number of experimental techniques have been employed to characterize solid/liquid interfaces and measure the associated surface charges. Among these are electrochemical techniques,[1] electrokinetic measurements,[2] surface charge titrations,[2b] and surface force apparatus (SFA)[3] measurements. In recent years, the AFM,[4] initially developed as an instrument for imaging both conducting and nonconducting substrates, has been employed to measure surface force and surface charge.[5] The advantage of this approach compared to SFA is the ability to extend these surface force and surface charge studies to a wider range of substrates without regard to size, structure, or transparency. In these AFM force measurements, a small sphere of silica (10−20 μm in diameter) is attached to a microfabricated cantilever to provide a larger tip area and a well-defined tip geometry, thus allowing for direct comparisons to theory. Recently, this technique has been used with control of the potential of the substrate; by using this in situ atomic force microscopy/electrochemical technique,[6] the electrical double layer can be probed at an electrode surface at nanometer resolution under potential control.

In a recent paper,[7] an electrochemically addressable self-assembled monolayer (SAM) was studied by this technique. A significant difference between the (effective) surface charge measured by AFM and the (real) surface charge determined from the cyclic voltammograms was found. An initial explanation for this discrepancy, tight ion binding at the interface, was given to account for the greatly reduced surface charge. In this work, another electrochemical technique, chronoamperometry, was used in situ with AFM force measurements at a gold electrode operating in the double-layer region where negligible faradaic current passes. Using chronoamperometry, the real surface charge can be obtained precisely by integration of the charging current. Hence, the surface charges from AFM measurements and from electrochemical measurements can be compared. A simple system was adopted in this study. The working electrode was Au; the electrolyte was 10^{-3} M $KClO_4$. There is no (or very weak) specific adsorption for $KClO_4$ on gold surfaces at very low electrolyte concentrations,[8] so that specific adsorption can be excluded, simplifying the data analysis. We show that the results again confirm the significant difference between the surface charges obtained by the AFM force curve and the electrochemical measurements. This great difference suggests that classical Guoy−Chapman−Stern theory does not adequately describe the electrical double layer at an electrode surface. More advanced models, e.g., those including ion correlation and ion condensation effects, can account for the reduced surface charge,

10.1021/jp003687i CCC: $20.00 © 2001 American Chemical Society
Published on Web 05/10/2001

as shown by a comparison of the experimental results found here and recent theoretical models.

Experimental Section

Materials. *Reagents.* $KClO_4$, Na_2SO_4, $Ca(NO_3)_2$, $NaNO_3$ and sodium dodecyl sulfate (SDS), all reagent-grade chemicals (Aldrich, Milwaukee, WI), were used as received. Solutions were prepared with 18 MΩ deionized water (Milli-Q Plus, Millipore Corp., Bedford, MA). Immediately before use, the solutions were deaerated with argon for 20 min. Typically, the unbuffered solutions showed a pH of 5.5−6.

Substrate Preparation. Silica substrates were prepared from commercial glass cover slips (M6045-2, Baxter Healthcare Corp., McGraw Park, IL). Before each experiment, the silica substrates were cleaned in piranha solution (a mixture of 70% H_2SO_4 and 30% H_2O_2) at ∼90 °C for 10 min. (*Caution: Piranha solution reacts violently with organic compounds and should be handled carefully.*) AFM imaging of the silica surfaces indicated a mean roughness of 1.1−1.4 nm/μm^2, with a maximum peak-to-valley height of 3.5−4.7 nm over a 1 μm × 1 μm area. Gold substrate electrodes were prepared by gluing a 2-mm-diameter gold wire (99.99%, Aldrich) with epoxy (Torr Seal, Varian) in a 3-mm-diameter hole in a 12-mm-diameter × 4-mm-thick glass disk. Electrical contact was then made with an insulated copper wire to the gold electrode through the back of the glass disk with conductive colloidal silver (Ted Pella Inc., Tustin, CA). Then, the gold/glass surface was fixed to a magnetic, stainless steel sample disk with epoxy (Torr Seal, Varian). The gold/glass surface was polished to optical smoothness with successive Carbimet papers and Al_2O_3 powder (1, 0.3, and 0.05 μm) (Buehler, Lake Bluff, IL). The polished gold surface had an electrochemically active area of 3.14 mm^2, and exhibited a mean roughness of 1−2 nm/μm^2, with a maximum peak-to-valley height of 7−9 nm over a 1 μm × 1 μm area. Immediately prior to use, the sample was polished with 0.05-μm Al_2O_3 for several minutes, rinsed with water, and dried under argon.

Electrochemistry. For in situ electrochemical measurements, experiments were carried out in an AFM liquid cell (Digital Instruments, Santa Barbara, CA) with Teflon tubing inlets and outlets. A three-electrode design was used in the electrochemical measurements, with the gold substrate serving as the working electrode, a Pt counterelectrode, and an Ag/AgCl wire immersed in the solution as the reference electrode. All electrode potentials are cited with respect to this Ag/AgCl wire reference. Electrochemical control of the cell was effected with a CHI-660 electrochemical workstation (CH Instruments, Austin, TX) under computer control. In the chronoamperometry experiments, the initial potential was set to the potential of zero charge (0.25 V vs Ag/AgCl for Au in 10^{-3} M $KClO_4$, determined as described below) and then stepped to potentials from −0.5 to 0.5 V. The double-layer charging current was recorded for each potential, and the surface charge was obtained by integrating the charging current curves. The differential capacitance curve for gold was obtained using the CHI-660 instrument in the ac voltammetry mode. The ac frequency was 10 Hz, with a peak-to-peak amplitude of 5 mV. The dc potential was scanned at a rate of 5 mV s^{-1} from positive to negative potentials in a 10^{-3} M solution of $KClO_4$.

AFM Force Measurement. Force measurements were performed with a Nanoscope III AFM (Digital Instruments) equipped with a piezo scanner having a maximum scan range of 15 μm × 15 μm × 2 μm. The standard AFM silicon nitride tip was modified by the attachment of a spherical silica bead. The AFM force measuring technique is well-documented,[5] and the experimental details have been described elsewhere.[6] The diameter of the silica spheres used was 10−20 μm. The *z* direction was calibrated by measuring the wavelength of the optical interference patterns resulting from reflection between the tip and a reflective substrate.[9] The spring constant of the silica sphere-modified cantilever, determined by the method of Cleveland et al.,[10] was 0.46−0.65 N/m. During the acquisition of a force curve, cantilever deflections were monitored by recording the changes in voltage at a split photodiode onto which was focused a laser beam that was reflected from the backside of the cantilever. The *z* direction displacement was given by the piezo scanner voltage. The raw data was converted to a normalized force (force/radius, F/R) vs tip−substrate separation for further analysis. Derjaguin−Landau−Verwey−Overbeek (DLVO) theory[11] was employed to calculate the (effective) surface potentials between the charged surfaces. The electrical-double-layer interaction energy was calculated for the constant-charge limit of the complete nonlinear Poisson−Boltzmann equation using the method of Hillier et al.[6] The Hamaker constants used for the theoretical calculations were 0.88×10^{-20} and 1.2×10^{-19} J for the silica−silica and silica−gold interactions, respectively. The surface potential of silica sphere, determined as in previous studies[5,6] by force measurements above a silica substrate, was −40 mV.

The AFM effective surface charge was calculated from the fitted (effective) potential at the OHP (measured by the AFM technique) with the formula[1]

$$\sigma^M = -\sigma^S = (8kT\epsilon\epsilon_0 n^0)\sinh\left(\frac{ze\psi_2}{2kT}\right)$$

Results and Discussion

CV of the Au Electrode. The CV of the Au electrode was carried out to locate the double-layer region of Au electrode under our experiment conditions, so that electrochemical charging of the double layer could be accomplished in the absence of significant faradaic charge passage. Repeated current−potential scans into regions of gold oxidation and reduction are also useful in cleaning the Au surface. The Au surface is easily contaminated, and cleanness of the Au surface is important for obtaining reliable and reproducible experimental results. Figure 1a shows the cyclic voltammogram of the first cycle of Au in 10^{-3} M $KClO_4$. One oxidative peak (0.92 V) and two reductive peaks (−0.11 and 0.41 V) appear. For the two reductive peaks, the intensity of the peak at −0.11 V increased, whereas the intensity of the peak at 0.41 V decreased as the number CV cycles increased. In our experiments the Au electrode was cycled from −0.6 to 1.2 V vs Ag/AgCl at 20 mV s^{-1} for about 20 min until a stable baseline was obtained. Figure 1b shows that the double-layer region of the Au electrode in 10^{-3} M $KClO_4$ extends from −0.6 to 0.5 V.

Force Curves of Au. Figure 2 shows the force curves between the negatively charged silica sphere and the gold electrode as a function of electrode potential in 10^{-3} M $KClO_4$. The force is repulsive at negative potentials. As the potential moves from negative potentials to positive potentials, the repulsive force decreases, and gradually attractive forces are observed. This result agrees well with our previous results on Au in NaF, KCl, KBr, and KI.[6] As noted earlier,[6] at the potential of zero charge, E_z, the Au electrode is uncharged, no diffuse double layer forms, and hence, the force between silica and gold is nearly zero. At potentials negative to E_z, the gold electrode is negatively charged and a repulsive force between silica and

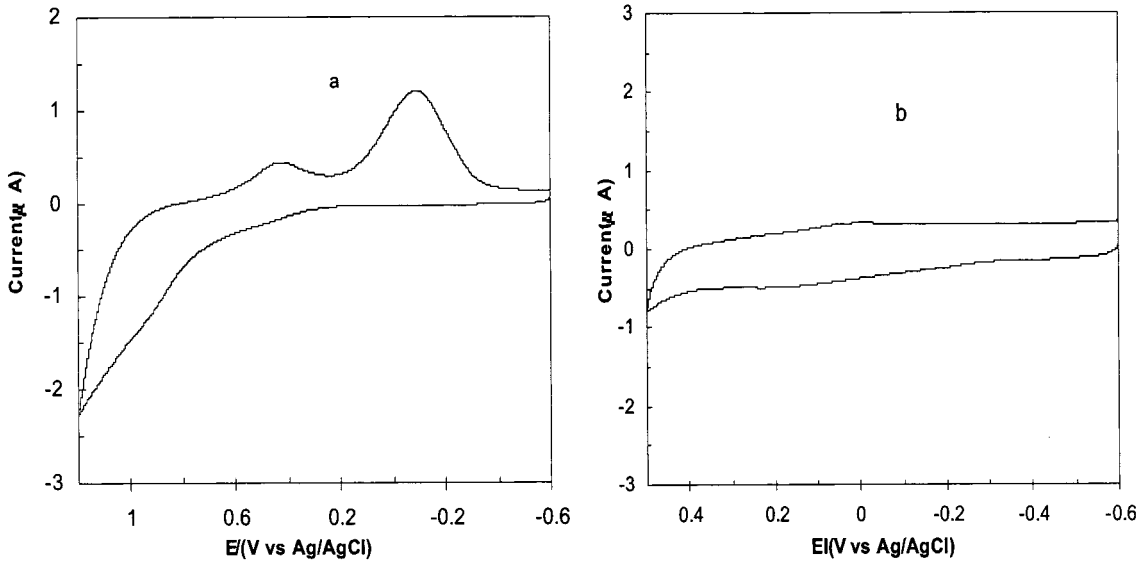

Figure 1. Cyclic voltammograms of Au in 10^{-3} M $KClO_4$: (a) scan rate = 0.02 V s^{-1}, (b) scan rate = 0.1 V s^{-1}.

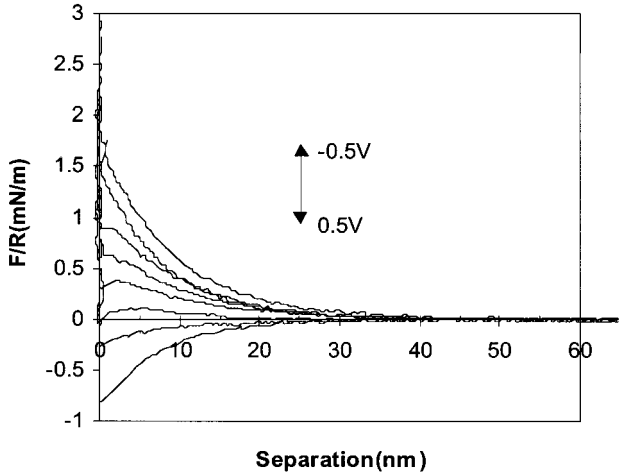

Figure 2. Forces between a silica probe and a Au electrode in 10^{-3} M aqueous $KClO_4$ at pH ~5.5 as a function of electrode potential. The force curves correspond to controlled potentials of, from top to bottom, −0.5, −0.3, −0.1, 0, 0.1, 0.2, 0.3, and 0.5 V vs Ag/AgCl.

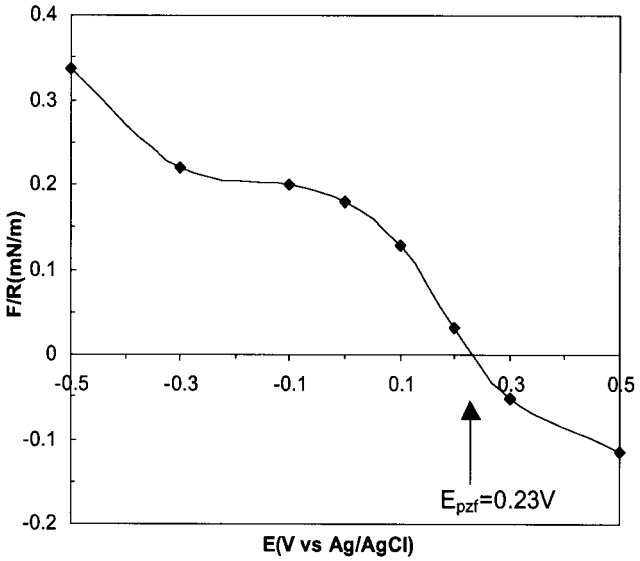

Figure 3. Force between a silica sphere and a gold electrode in 10^{-3} M $KClO_4$ solution at a fixed separation of 15 nm as a function of electrode potential.

gold is obtained. When the potential of the gold electrode is positive with respect to E_z, the electrode is positively charged, and an attractive force between silica and gold is observed. Therefore, the potential of zero force corresponds to E_z. Figure 3 shows the force between the silica sphere and the gold electrode in 10^{-3} M $KClO_4$ at a fixed separation of 15 nm as a function of electrode potential. From this figure, the potential of zero force is found to be about 0.23 V vs Ag/AgCl.

The diffuse double layer reflects the magnitude of the surface charge of the substrate immersed in a solution. Methods for fitting the force between interacting double layers in electrolytic solutions using Poisson−Boltzmann theory have been well-developed. In this work, the method of Hiller et al.[6] was used to find the effective surface potential, and hence the effective surface charge, of the electric double layer between the interacting surfaces. The effective surface potential and surface charge of the Au electrode in 10^{-3} M $KClO_4$ at different potentials are listed in Table 1. For attractive forces, the cantilever is unstable[12] and tends to jump to contact, which prevents accurate measurement of attractive forces. Thus, only surface potentials and surface charges corresponding to repulsive forces are listed in Table 1. Figure 4 shows the differential capacitance of Au in 10^{-3} M $KClO_4$ obtained by the ac

TABLE 1: Effective ψ_2 Potential and Effective/Real Surface Charges for Au in 10^{-3} M $KClO_4$ at Different Potentials

potential (V vs Ag/AgCl)	ψ_2 (mV)	real surface charge (μC/cm^2)	effective surface charge (μC/cm^2)	effective surface charge/real surface charge
−0.5	−76	−20.4	−0.772	0.038
−0.3	−58	−12.6	−0.514	0.041
−0.1	−47	−6.94	−0.389	0.056
0	−40	−4.98	−0.319	0.064
0.1	−34	−3.09	−0.229	0.074
0.2	−16	−1.08	−0.102	0.095

voltammetric method. The values of the differential capacitance (C_d) shown are based on the geometric (projected) area of the electrode. The minimum value of C_d, ~15 μF/cm^2, is generally taken to correspond to E_z. The value found for E_z is 0.27 V vs Ag/AgCl, which is close to the potential of zero force (0.23 V). We take $E_z = 0.25 \pm 0.03$ V vs Ag/AgCl.

Chronoamperometry Experiments. In the potential step experiments, the potential was initially set to E_z and then stepped to different values in the double layer region, and the resulting current−time transient recorded. Figure 5 shows these transients

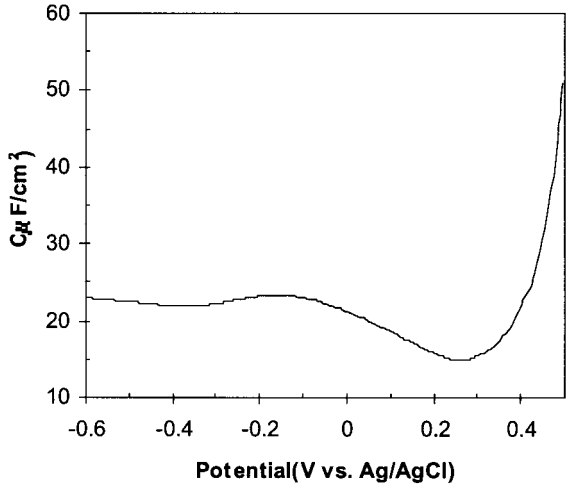

Figure 4. Differential capacitance of a gold electrode in 10^{-3} M $KClO_4$ solution.

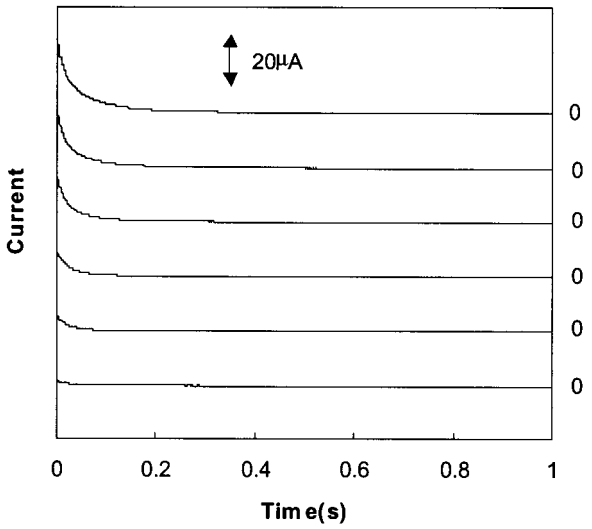

Figure 5. Current−time transients of a Au electrode in 10^{-3} M $KClO_4$ in chronoamperometry experiments. The initial potential is 0.25 V; the final potential, from top to bottom, is −0.5, −0.3, −0.1, 0, 0.1, and 0.2 V vs Ag/AgCl.

at different final potentials over a 1-s time window. The currents decay exponentially with time in a strict way, which again confirms that these currents are due to the charging of the electric double layer of the Au electrode. An analysis of these curves is consistent with a double-layer capacitance of 43 μF/cm^2 and an uncompensated resistance of 25 kΩ. By stepping the potential back to E_z, one can obtain the discharge transients. Even when the step time is increased to 2 min, there is no apparent change of the discharge current. This demonstrates that the charge on the electrode is stable for a period of at least 2 min. The results of the electrochemical surface charge (normalized to unit area in square centimeters) at different potentials from the integration of the current−time curves are summarized in Table 1. To normalize these data, the real area or surface roughness factor of the Au electrode must be known. In our experiments, a polished Au electrode is used. Bruckenstein et al. systematically studied the effects of polishing Au electrodes with different-sized abrasives.[13] For a smooth, well-polished gold electrode using 0.05-μm alumina abrasive, the surface roughness factor ranges from 1.5 to 2.05. In our case, we choose a value of 1.6 as the surface roughness factor of the polished Au electrode.[14]

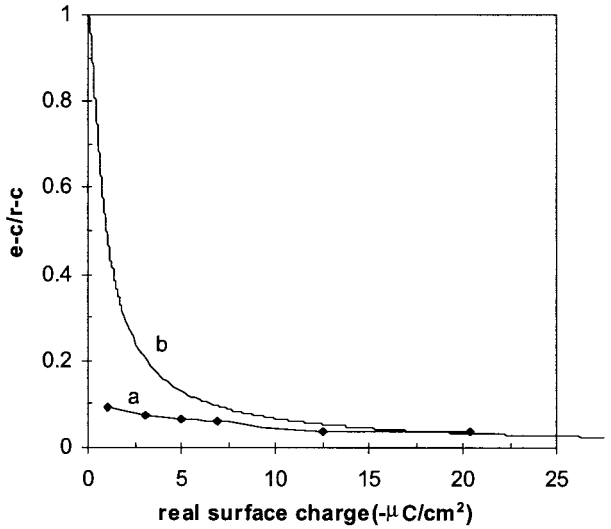

Figure 6. Ratio of the effective/real surface charge for Au electrode in 10^{-3} M $KClO_4$ solution: (a) experimental results, (b) theory (Attard[21]).

Electrochemical (Real) vs AFM (Effective) Surface Charge. There is a large difference between the effective (AFM) and real (electrochemical) surface charge, as shown in Table 1 and, more clearly, in the fraction of the effective/real surface charge as a function of real charge depicted in Figure 6. Typically, the effective surface charge is only a few percent of the real surface charge. This result is in agreement with our previous results, which showed that the surface charge obtained by fitting the force curve using Poisson−Boltzmann theory was much less than that obtained by cyclic voltammograms in electrochemically addressable self-assembled monolayers.[7]

Although this large difference between the effective and real surface charge on an electrode surface seems surprising, this same phenomenon is found frequently for many types of interfaces. In fact, to the best of our knowledge, the surface potentials obtained by force measurements are almost below 120 mV in 10^{-3} M electrolyte, independent of the surface used, implying that the surface charges obtained by force measurements are almost always below 1.90 μC/cm^2. This is only a few percent of the total amount of charge on many surfaces, ca. 20−30 μC/cm^2. In colloid chemistry, the surface charges, as obtained by ζ-potential measurements in electrokinetic experiments, are known to be much lower than those found by surface charge titrations.[2b] Note that almost all of the surface charge data available in the literature, e.g., by surface force measurements or electrokinetic experiments, are based on Gouy−Chapmann−Stern (GCS)[18] theory of the electrical double layer. The conclusion from our experiments, as well as earlier colloid measurements, is that one cannot obtain a good estimate of the diffuse double-layer charge via GCS theory.

Although GCS theory has been extensively used to describe the electrical double layer in electrochemistry, colloidal chemistry, and biochemistry, the validity of GCS theory is still in dispute. Many approximations are included in classical GCS theory, such as the point charge, hard wall model, and dielectric continuum approximations. A key issue in GCS theory is the use of the Poisson−Boltzmann (PB) equation, which implies a mean-field method that takes the density of ions in the double layer near the charged surface to be proportional to the Boltzmann factor with the average electrostatic potential, which is, in turn, related to the ion density by Poisson's equation.

Over the past several decades, there have been many attempts to explain the reduced surface charge, e.g., the porous double-

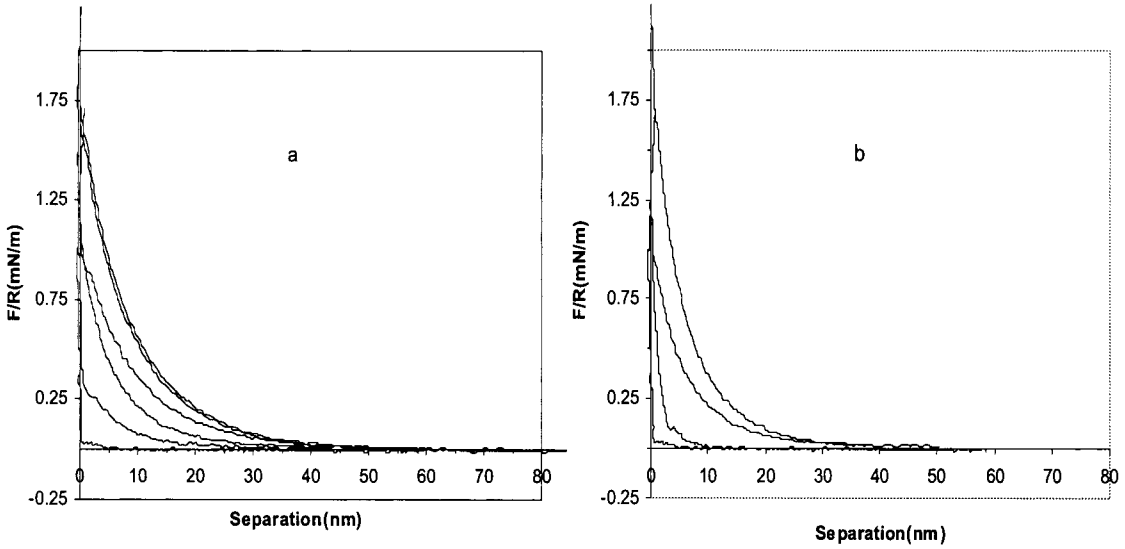

Figure 7. Force curves of silica−silica interactions at pH ∼5.5 in divalent electrolytes. (a) In different mixture solutions of $Ca(NO_3)_2$ and $NaNO_3$. From top to bottom: 10^{-3} M $NaNO_3$, 10^{-5} M $Ca(NO_3)_2$ + 10^{-3} M $NaNO_3$, 10^{-4} M $Ca(NO_3)_2$ + 0.86×10^{-3} M $NaNO_3$, 0.7×10^{-3} M $Ca(NO_3)_2$, 10^{-3} M $Ca(NO_3)_2$, 10^{-2} M $Ca(NO_3)_2$. (b) Comparison of $Ca(NO_3)_2$ with Na_2SO_4. From top to bottom: 0.7×10^{-3} M Na_2SO_4, 0.7×10^{-3} M $Ca(NO_3)_2$, 10^{-2} M Na_2SO_4, and 10^{-2} M $Ca(NO_3)_2$.

layer model,[15] the porous double-layer model combined with ionizable surface groups,[16] and the gel layer assumption.[17] Although some of these can be used in specific cases, they do not account for the observed discrepancy in surface charge. In addition to the above attempts to modify classical GCS theory, there have been other studies that include effects not in classical GCS theory. Of all such effects, ion correlation/ion condensation effects might be of the greatest importance. In PB theory, the effect of ion−ion correlation is neglected. As pointed out by Kjellander et al.,[19a,b] there are several consequences of ion−ion correlations: (1) Compared to the results from PB theory, more ions are allowed closer to the walls because the region between each ion and the closest wall is, on average, depleted of other ions. (2) The gathering of ions closer to the walls leads to a lowering of the concentration at the midplane between the surfaces and, hence, to a less repulsive contribution to the interaction between the surfaces. Generally speaking, because of ion correlation, more counterions are "condensed" at the solid surface, thus leading to a reduced surface charge. This kind of ion condensation is equivalent to a nonspecific electrostatic "adsorption" of ions to the surface.

Ion correlation/ion condensation effects have often been proposed to describe the electrical double layer. Manning proposed such a concept to account for the condensation of counterions onto polyions.[20] Kjellander et al.[19] and Attard et al.[21] suggested use of the effective surface charge to describe a reduced surface charge based on ion condensation. More recently, Chen et al. showed computationally that ion condensation near charged colloidal particles leads to a reduced electrostatic interaction between the particles.[22] However, there have been few experimental studies testing such an effect.[23] In general, it is difficult to measure experimentally effective and real surface charge at the same time, especially at electrode/solution interfaces. Our results can be interpreted in terms of such ion correlation/ion condensation effects. Recently, Attard et al. proposed a convenient analytical expression that is based on the extended Poisson−Boltzmann approximation and the concept of ion correlation for converting effective surface charge, $\bar{\sigma}$ (calculated from GC theory), to the actual surface charge, σ.[21] Using the analytical expression (eq 8a in ref 21), we calculated the effective/real surface charge ratio at different real surface charges for a 1 mM $KClO_4$ solution. The results are depicted in Figure 6. Both the experimental and theoretical values show the same trend, that is, the effective/real surface charge ratio decreases as the real surface charge density increases. At high surface charge densities, the theoretical values converge quite well with experimental values. The effective/real surface ratio decreases to a very small value, ca. 3%. As the surface charge decreases, the effective/real surface charge ratio increases. However, the experimental ratio increases much more slowly than that predicted by theory. Even at a quite low surface charge density (-1.08 $\mu C/cm^2$), the experimental ratio was only about 10%, far below the theoretical value of 74%. At present, it is unclear why there is such a significant difference between the experimental effective surface charge and the theoretical values, even at low surface charge densities. Perhaps ion pairing at the interface must also be taken into account.[24]

Divalent Electrolytes. To further investigate the ion correlation/ion condensation effect, we performed the same experiments with a +2 cation, Ca^{2+}. Theoretically, in a divalent electrolyte, electrostatic correlations should be larger than those in a monovalent electrolyte.[21] We designed a routine to test the effect of the divalent electrolyte. We studied the silica−silica interaction with different divalent concentrations while (in some cases) maintaining a constant total concentration of the electrolyte. The results are given in Figure 7. In a mixed electrolyte of 10^{-5} M $Ca(NO_3)_2$ and 10^{-3} M $NaNO_3$, the force is slightly lower than that in pure 10^{-3} M $NaNO_3$ solution. When the concentration of $Ca(NO_3)_2$ increases, the force decreases, as predicted by the theory. With a different divalent electrolyte, Na_2SO_4, similar results were obtained (Figure 7b). For forces at electrolytes of the same concentration between $Ca(NO_3)_2$ and Na_2SO_4, the force with $Ca(NO_3)_2$ is much lower than that with Na_2SO_4, which again is consistent with the condensation of the divalent cation at the negatively charged surface.

Effect of Surfactant. The adsorption of surface-active substances on the gold surface can occur through exposure to adventitious impurities in the air or solution and can affect the observed AFM response. Moreover, the nature of ion condensation with an organic anion might be different than that with ClO_4^-. To investigate this effect, experiments with sodium dodecyl sulfate (SDS) on the gold electrode were performed.

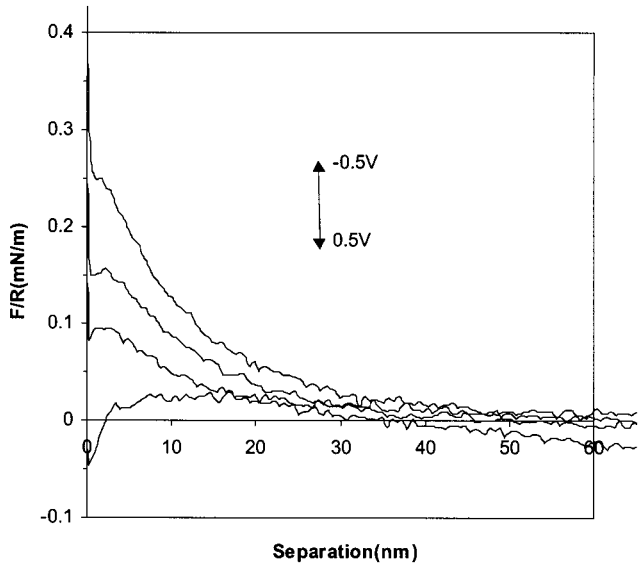

Figure 8. Force between a silica probe and a Au electrode at pH ~5.5 as a function of electrode potential. The total salt concentration (C_{SDS} + C_{KClO_4}) was 10^{-3} M. The SDS concentration is 10^{-5} M. The force curves correspond to controlled potentials of, from top to bottom, −0.5, −0.3, 0.1, and 0.5 V vs Ag/AgCl.

A mixture of $KClO_4$ and SDS solution, with the total salt concentration maintained at 10^{-3} M and with the SDS concentration varying from very low to higher values, was employed (Figure 8). When the SDS concentration was 10^{-7} M, the measured force curve was identical to that obtained from a $KClO_4$ solution without SDS. At a SDS concentration of 10^{-6} M, there is a slight decrease of force (data not shown). When the concentration of SDS increased to 10^{-5} M, there was a large decrease in the force, demonstrating a strong effect of surfactant.

Many studies on the adsorption of surfactants on solid/liquid interfaces, mainly on oppositely charged surfaces, have been reported.[25] Fewer studies have been conducted on the adsorption of surfactants on similarly charged surfaces. In our case, the anionic SDS surfactant adsorbed on a negatively charged gold surface and decreased the force. This might be ascribed to an increase in ion pairing between the condensed cations and the anionic SDS because of the change in the solution environment near the electrode surface. For example, the effective dielectric constant of the interfacial region could be smaller because of the surfactant, thus leading to a greater level of cation condensation. This would lead to a reduction in the force between the silica and Au surfaces. Recently, Kreisig et al. used FT-SERS to study the adsorption of cetylpyridinum bromide (CTPB) on a silver surface.[26] They also proposed the same condensation of a layer of counterions near the CTPB on a charged silver surface. This is consistent with the model proposed here.

Conclusions

The surface charge at solid/liquid interfaces has been measured for Au in $KClO_4$ solution using an in situ atomic force microscopy/electrochemistry technique. A large difference between the real surface charge (from electrochemistry) and the effective surface charge (from AFM) was observed. An ion correlation/ion condensation effect was proposed to account for the reduced surface charge, and evidence for such an effect was presented. The results suggest the failure of classical Guoy−Chapman−Stern theory to describe the electrical double layer and the importance of ion correlation/ion condensation effects at electrode surfaces.

Acknowledgment. The support of this research by the National Science Foundation (CHE-9870762) and the Robert A. Welch Foundation is gratefully acknowledged. The authors thank Professor Andrew C. Hillier (University of Virginia) for developing the computer program for the calculation of double-layer forces and Professor Peter Rossky (University of Texas at Austin) for helpful discussions concerning this work.

References and Notes

(1) (a) Grahame, D. C. *Chem. Rev.* **1947**, *41*, 441. (b) Parsons, P. In *Modern Aspects of Electrochemistry*; Bockris, J. O'M., Ed.; Academic Press: New York, 1954. (c) Delahay, P. *Double Layer and Electrode Kinetics*; Wiley-Interscience: New York, 1965; Chapter 2. (d) Mohilner, D. M. In *Electroanalytical Chemistry*; Bard, A. J., Ed.; Marcel Dekker: New York, 1966; Vol. 1. (e) Bard, A. J.; Faulkner, L. R. *Electrochemical Methods: Fundamentals and Applications*, 2nd ed.; John Wiley and Sons: New York, 2001; Chapter 13.

(2) (a) Hunter, R. J. *Foundations of Colloid Science I*; Clarendon Press: London, 1989; Chapter 9. (b) Hunter, R. J. *Introduction to Modern Colloid Science*; Oxford University Press: New York, 1993; Chapter 8. (c) *Handbook of Surface and Colloid Chemistry*; Birdi, K. S., Ed., CRC Press: Boca Raton, FL, 1997; Chapter 11.

(3) (a) Israelachvili, J. N.; Adams, G. E. *J. Chem. Phys.* **1978**, *74*, 975. (b) Isrealachvili, J. N.; Adams, G. E. *J. Chem. Phys.* **1981**, *75*, 1400.

(4) Binning, G.; Quate, C.; Gerber, G. *Phys. Rev. Lett.* **1986**, *56*, 930.

(5) (a) Ducker, W. A.; Senden, T. J.; Pashley, R. M. *Nature* **1991**, *353*, 239. (b) Ducker, W. A.; Senden, T. J.; Pashley, R. M. *Langmuir* **1992**, *8*, 1831.

(6) Hiller, A. C.; Kim, S.; Bard, A. J. *J. Phys. Chem.* **1996**, *100*, 18808.

(7) Hu, K.; Bard, A. J. *Langmuir* **1999**, *15*, 3343.

(8) Clavier, J.; Van Huong, C. N. *J. Electroanal. Chem.* **1977**, *80*, 101.

(9) Jasche, M.; Butt, H.-J. *Rev. Sci. Instrum.* **1995**, *66*, 1258.

(10) (a) Cleveland, J. P.; Manne, S.; Bocek, D.; Hansma, P. K. *Rev. Sci. Instrum.* **1993**, *64*, 403. (b) Sader, J. E.; Larson, I.; Mulvaney, P.; White, L. R. *Rev. Sci. Instrum.* **1995**, *66*, 3789.

(11) (a) Derjaguin, B. *Trans. Faraday Soc.* **1940**, *36*, 203. (b) Derjaguin, B. V.; Landau, L. D. *Acta Phys. Chem.* **1941**, *14*, 633. (c) Derjaguin, B. V.; Landau, L. D. *J. Exp. Theor. Phys.* **1941**, *11*, 802. (d) Verwey, E. J. W.; Overbeek, J. T. G. *Theory of the Stability of Lyophobic Colloids*; Elsevier: New York, 1948.

(12) Israelachvili, J. N. *Intermolecular and Surface Forces*, 2nd ed.; Academic Press: New York, 1991.

(13) Bruckenstein, S.; Sharkey J. W.; Yip, J. Y. *Anal. Chem.* **1985**, *57*, 371.

(14) There is some error involved in estimating the surface roughness factor of the Au electrode. However, as shown later, because there is such a great difference between the effective and real surface charge, the error does not affect our conclusions.

(15) (a) Lyklema, J. *J. Electroanal. Chem.* **1968**, *18*, 341. (b) Lyklema, J. *Croat. Chem. Acta* **1971**, *43*, 249.

(16) Kleijn, J. M. *Colloids Surf.* **1990**, *51*, 371.

(17) Perramm J. W.; Hunter, R. J.; Wright, H. J. L. *Aust. J. Chem.* **1974**, *27*, 461.

(18) (a) Gouy, G. *J. Phys. Radium* **1910**, *9*, 457. (b) Gouy, G. *Compt. Rend.* **1910**, *149*, 654. (c) Chapman, D. L. *Philos. Mag.* **1913**, *25*, 475. (d) Stern, O. *Z. Elektrochem.* **1924**, *30*, 508.

(19) (a) Kjellander R.; Marelja S. *J. Phys. Chem.* **1986**, *90*, 1230. (b) Ennis, J.; Marelja, Kjellander, R. *Electrochim. Acta* **1996**, *41*, 2115.

(20) (a) Manning, G. S. *J. Chem. Phys.* **1969**, *51*, 924. (b) Manning, G. S. *Acc. Chem. Res.* **1979**, *12*, 443.

(21) (a) Attard, P. *J. Phys. Chem.* **1995**, *99*, 14174. (b) Attard, P. In *Advances in Chemical Physics*; John Wiley and Sons: New York, 1996; Vol. XCII.

(22) Chen, P. L.; Lu, C.-Y. D. *Phys. Rev. E* **2000**, *61*, 824.

(23) A recent paper has been written on ion condensation on charged particles: Fernandez-Nieves, A.; Fernandez-Barbero, A.; de las Nieves, F. J. *Langmuir* **2000**, *16*, 4090. The fraction of condensed ions is ca. 90%, which is similar to our results.

(24) Kane, V.; Mulvaney, P. *Langmuir* **1998**, *14*, 3303.

(25) For example, see: (a) Somasundaran, P.; Fuerstenau, D. W. *J. Phys. Chem.* **1966**, *70*, 90. (b) Harwell, J. H.; Hoskins, J. C.; Schechter, R. S.; Wade, W. H. *Langmuir* **1985**, *1*, 251. (c) Gu, T.; Huang, Z. *Colloids Surf.* **1989**, *40*, 71. (d) Böhmer, M. R.; Koopal, L. K. *Langmuir* **1992**, *8*, 2649. (e) Hu, K.; Bard, A. J. *Langmuir* **1997**, *13*, 5418.

(26) Kreisig, S. M.; Tarazona, A.; Koglin, E.; Schwuger, M. J. *Langmuir* **1996**, *12*, 5279.